

Review

Non-Volatile Particle Number Emission Measurements with Catalytic Strippers: A Review

Barouch Giechaskiel ^{*}, Anastasios D. Melas , Tero Lähde and Giorgio Martini

European Commission—Joint Research Centre (JRC), 21027 Ispra, Italy; anastasios.melas@ec.europa.eu (A.D.M.); tero.lahde@ec.europa.eu (T.L.); giorgio.martini@ec.europa.eu (G.M.)

^{*} Correspondence: barouch.giechaskiel@ec.europa.eu; Tel.: +39-0332-78-5312

Received: 21 May 2020; Accepted: 23 June 2020; Published: 24 June 2020



Abstract: Vehicle regulations include limits for non-volatile particle number emissions with sizes larger than 23 nm. The measurements are conducted with systems that remove the volatile particles by means of dilution and heating. Recently, the option of measuring from 10 nm was included in the Global Technical Regulation (GTR 15) as an additional option to the current >23 nm methodology. In order to avoid artefacts, i.e., measuring volatile particles that have nucleated downstream of the evaporation tube, a heated oxidation catalyst (i.e., catalytic stripper) is required. This review summarizes the studies with laboratory aerosols that assessed the volatile removal efficiency of evaporation tube and catalytic stripper-based systems using hydrocarbons, sulfuric acid, mixture of them, and ammonium sulfate. Special emphasis was given to distinguish between artefacts that happened in the 10–23 nm range or below. Furthermore, studies with vehicles' aerosols that reported artefacts were collected to estimate critical concentration levels of volatiles. Maximum expected levels of volatiles for mopeds, motorcycles, light-duty and heavy-duty vehicles were also summarized. Both laboratory and vehicle studies confirmed the superiority of catalytic strippers in avoiding artefacts. Open issues that need attention are the sulfur storage capacity and the standardization of technical requirements for catalytic strippers.

Keywords: vehicle emissions; particle measurement programme (PMP); portable emissions measurement systems (PEMS); volatile removal efficiency; non-volatiles; solid particle number; catalytic stripper; evaporation tube; artefact

1. Introduction

In order to reduce pollution from particulate matter (PM), limits for the PM mass emissions of vehicles are applicable in most countries worldwide [1]. The engine and aftertreatment improvements reduced the emitted PM levels close to the detection limit of the PM methodology [2]. In order to further control the emissions of ultrafine particles, which do not contribute significantly to the PM mass, the European Union (EU) regulations included limits for the non-volatile particle emissions of light-duty, heavy-duty, and non-road mobile machinery since 2011–2013 [3,4].

The particle number methodology is based on sampling from a dilution tunnel where the whole exhaust gas is mixed with ambient air dilution air. In order to measure only non-volatile particles, the sample is pre-conditioned first in a hot diluter at 150 °C and then in an evaporation tube at 350 °C, the so called volatile particle remover [5,6]. After a secondary dilution at ambient temperature, a particle number counter (PNC) counts all (non-volatile) particles above 23 nm. In reality the detection efficiency of the PNC, typically a condensation particle counter (CPC), is around 50% at 23 nm, >90% at 41 nm and 0% at 17 nm. The 23 nm cut-off size was selected in order to include the smallest primary soot particles, and exclude the volatile nucleation mode particles that could survive the pre-conditioning unit. The methodology was extended, but more simplified, to measure directly from

the tailpipe during on-road tests with the real-driving emissions (RDE) regulation for both light-duty and heavy-duty vehicles [7]. The portable emissions measurement systems (PEMS) set the volatile particle remover at 300 °C, in order to reduce energy consumption. From the controlled laboratory environment, the measurements can take place under any environmental and driving conditions, thus the measurement equipment can be challenged. Indeed, the survival of volatile particles through the thermal pre-conditioning unit or formation of volatile particles after the unit can lead to false high concentrations of volatiles that will be counted as non-volatile particles. This was quite unlikely with the 23 nm cut-off size of the PNC, but has happened in the sub-23 nm range [8,9], raising concerns as to whether the methodology should be extended below 23 nm.

On the other hand, a major criticism of the particle number methodology is that it excludes an important fraction of non-volatile particles below 23 nm that are emitted by many vehicle technologies [10]. For example, sub-23 nm non-volatile particles have been reported for heavy-duty vehicles [11], especially during urea injection [12], gasoline fueled vehicles [13], both port-fuel and direct injection vehicles. Recently, concerns for CNG (compressed natural gas) fueled vehicles were also raised [3,12]. Mopeds and motorcycles have also a high percentage of sub-23 nm particles. For this reason, the intention is to extend the methodology to include particles from approximately 10 nm. The 10 nm size was selected in order to permit the upgrade of existing PN systems without investment costs and to minimize the higher risk of surviving (or re-nucleating) volatile particles [14]. Furthermore, it will be suitable for the upgrade of the current 23 nm PEMS [15,16]. Developing a methodology to count smaller than 10 nm particles would be extremely challenging due to the uncertainties related to particle losses and calibration procedures.

A proposed methodology to eliminate the volatiles and make the methodology more robust is the catalytic stripper [17]. The idea is based on catalytic converters of vehicles, which remove hydrocarbons (in addition to CO and NO_x). Typically, they utilize a ceramic honeycomb monolithic substrate (support) with many small parallel channels. The monolith walls are coated with an active catalyst layer [18]. The catalytic coating includes noble metal catalysts (such as Pt and Pd) impregnated on a porous high surface area layer of inorganic carrier (support), the washcoat, such as alumina and silica. The support material often contains additives such as promoters and stabilizers. Based on NO_x storage catalysts [19,20], the catalytic strippers include sometimes a sulfur trap to further improve their removal efficiency of sulfuric acid containing aerosol. Catalytic strippers have been used not only in the automotive field [21], but also in the aviation field [22], and for atmospheric measurements [23].

Thermodenuders can also remove volatiles species from the exhaust gas [24,25]. In the thermodenuders, the sample is first heated in an evaporation tube, and then it passes through an unheated section containing adsorbing material, most often activated carbon, which adsorbs most of the evaporated components.

The objective of this study is to review the volatile removal efficiency and sulfur storage capacity of catalytic strippers and their suitability for inclusion in the particle number systems. The review results are compared with the current methodology that uses hot dilution and evaporation tube and with thermodenuders used in research. In order to put the results into the right context, actual volatile emission levels from vehicles are also summarized. Finally, recommendations for technical requirements for catalytic strippers are proposed.

2. Materials and Methods

This review focused on studies that characterized catalytic strippers and evaporation tubes as standalone systems or in volatile particle removers of particle number systems (i.e., downstream of a hot dilution at temperature >150 °C). We searched in Google Scholar with keywords “catalytic stripper”, “evaporation tube + particles” and “volatile removal efficiency”. The search resulted in 533, 900 and 73 documents, respectively. From the abstracts it was decided whether the documents were relevant or not. The only acceptance criterion was the inclusion in the text of volatile removal efficiency with laboratory aerosols or vehicles’ exhaust. Studies that used evaporation tubes or catalytic strippers

for measurements of vehicle exhaust were excluded, unless there was discussion of possible artefacts, or comparisons between catalytic strippers and evaporation tubes on the removal of volatile particles. In total, 29 studies were selected, 18 used a laboratory aerosol, and 14 a vehicle's aerosol (3 were in common). Table 1 summarizes the studies included.

Table 1. Number of studies assessing evaporation tubes (ET), catalytic strippers (CS), or thermodenuders (TD). The laboratory studies were conducted with hydrocarbons (HCs) and/or sulfuric acid (H_2SO_4). In brackets the studies using CS with sulfur trap.

System	Laboratory HCs	Laboratory H_2SO_4	Vehicles' Aerosol
ET	13	6	14
CS	15 (9)	7 (5)	8 (7)
CS vs. ET or TD	10 (6)	6 (4)	8 (7)

We used the same search engine for sulfur storage capacity of catalysts and SO_2 to SO_3 conversion rates. Keywords such as “sulfur trap”, sulfur storage catalyst”, “sulfur absorber”, “sulfur poisoning” were used. Only key studies were used because the objective was to put the catalytic stripper assessment results into perspective (i.e., compare with automotive catalytic converters).

We also reviewed emission levels of volatile and semi-volatile components at the tailpipe of the vehicles or at the dilution tunnel. The focus was on two-stroke mopeds, motorcycles, gasoline and diesel light-duty and heavy-duty vehicles mainly of recent technologies. Special attention was paid to emission levels during the cold start of the engines, filter regenerations, or prolonged highway operation, where high levels of volatiles are expected. The search was narrowed to hydrocarbons, SO_2 , SO_3 and H_2SO_4 , which were the species that were used for the evaluation of the catalytic strippers and evaporation tubes. The research was not extensive, as the target was to find typical maximum levels that the particle number systems can be challenged.

3. Results

The particle number systems measure non-volatile particles >23 nm. Note that “solids” or “non-volatile” particles are by definition the particles that remain after thermal pre-treatment at 350 °C for a residence time of approximately 0.2–0.4 s. The term “volatiles” in this text covers all species that are in gaseous state at temperatures below 350 °C. More appropriate terms such as semi-volatile or intermediate volatility compounds will not be used [26].

3.1. Volatile Particle Remover

The particle number systems consist of a volatile particle remover (VPR) and a particle number counter (PNC). Figure 1 presents a volatile particle remover with an evaporation tube (upper panel) or a catalytic stripper (lower panel).

3.1.1. Evaporation Tube-Based Systems

The exhaust gas at the dilution tunnel is already diluted and cooled down to ambient temperature levels (usually between 20 °C and 50 °C). The diluted aerosol typically consists of soot particles with some species condensed on them, volatile nucleation mode particles, and volatile species in the gas phase. The volatile particles contain high percentages of compounds such as organics and sulfuric acid [27]. The soot particles are aggregates consisting of primary soot particles having diameters between 20 nm and 30 nm [28]. The geometric mean diameter of the soot mode is around 50–70 nm [2], but for modern gasoline engines, means of around 30 nm have also been reported [4]. The nucleation mode size-range is usually below 20 nm.

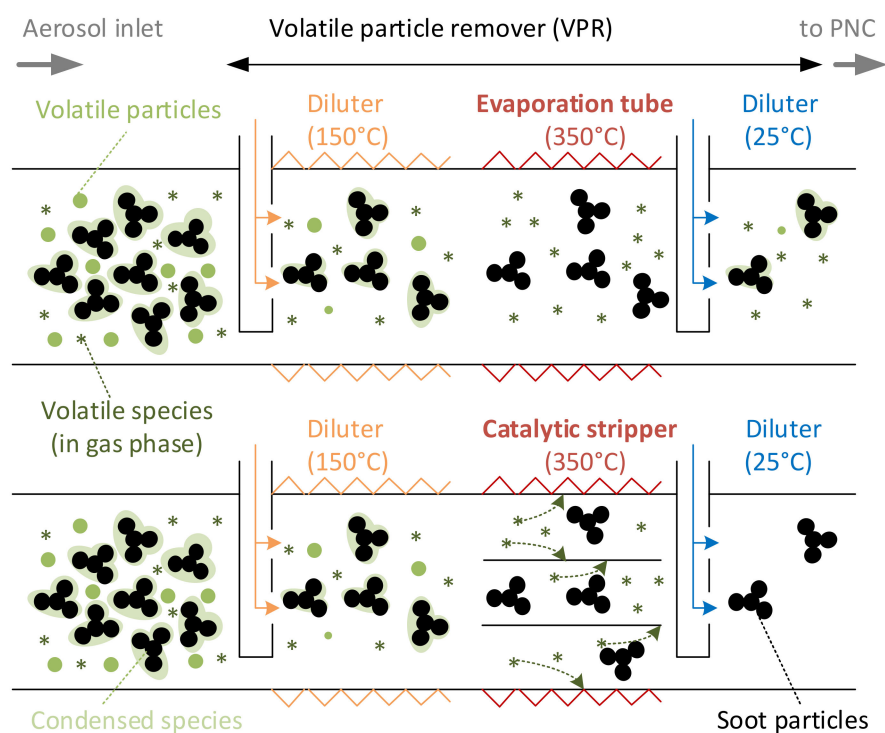


Figure 1. Schematic of volatile particle removers based on evaporation tube (upper panel) and catalytic stripper (lower panel). PNC = particle number counter.

In the primary hot diluter ($\geq 150\text{ }^{\circ}\text{C}$) some of the condensed material evaporates and the nucleation mode particles evaporate and shrink. Furthermore, the concentration (and partial pressure) of the volatile species decreases. In the evaporation tube ($350\text{ }^{\circ}\text{C}$) most of the volatile particles and the condensed material evaporate. The cold diluter downstream of the evaporation tube further dilutes the sample to bring the temperature and the soot concentration to an appropriate range for the PNC. During this process it is possible to have re-condensation on the soot particles and/or re-nucleation of volatile species (i.e., formation of new volatile particles) especially if the dilution ratio is not sufficiently high. The nucleated particles due to the low concentrations of available species are unlikely to grow over 23 nm in diameter, and thus they will not be counted by the PNC, which has detection efficiency of 50% for particles of 23 nm diameter. The particles nucleated downstream of the evaporation tube and counted with a PNC are called volatile artefacts [14]. The next sections will summarize the studies that evaluated the concentration levels of volatile species that artefacts can be avoided.

3.1.2. Catalytic Stripper-Based Systems

When a catalytic stripper is used, instead (or in addition to) an evaporation tube, the volatile species in the gas phase are oxidized (Figure 1, lower panel). Then, during dilution and cooling at the secondary diluter the concentrations of nucleating species is too low to form volatile particles and, thus, the possibility for artefacts is minimized.

There are three types of catalytic strippers. Those that comprise:

- Only oxidation catalyst;
- Sulfur trap and oxidation catalyst (in this order);
- Oxidation catalyst and sulfur trap.

The first catalytic stripper for automotive use was mentioned in 1995 [17]. It was constructed from a commercial diesel oxidation catalyst (DOC) and operated at $300\text{ }^{\circ}\text{C}$. A cooling coil tube downstream of the catalytic stripper reduced the sample temperature to ambient levels. Optimization work in terms of particle losses and volatile removal efficiency was presented in 2007 [29]. In particular, a vortex

tube diluter downstream of the catalytic stripper minimized thermophoretic losses. Later the catalytic stripper was installed in a particle number system compliant with the European regulations replacing the evaporation tube [30].

A catalytic stripper with an upstream sulfur trap was presented in 2003 [31]. The sulfur trap prevented poisoning of the oxidation catalyst by trapping the sulfur species and minimized artefacts from the nucleation of SO₃. This concept was compared to a thermodenuder in 2010 [32]. Later the position of the sulfur trap was assessed at a different catalytic stripper and it was found to have higher sulfur storage capacity when placed downstream [33]. The majority of the catalytic strippers in the market for research or regulation purposes consist either only of an oxidation catalyst or oxidation catalyst with a sulfur trap downstream.

3.2. Hydrocarbons

Figure 2 summarizes the volatile removal efficiency of studies that used hydrocarbons (tetracosane C₂₄, octacosane C₂₈, tetracontane C₄₀ and emery oil) for evaporation tube [5,30,32,34–43] and catalytic stripper-based [30,32–41,44–47] systems. Each point is a test. The mass concentration of the challenge aerosol can be seen in the *y*-axis. The *x*-axis is divided in four areas which indicate whether no or some particles remained (or nucleated) downstream of the system under evaluation.

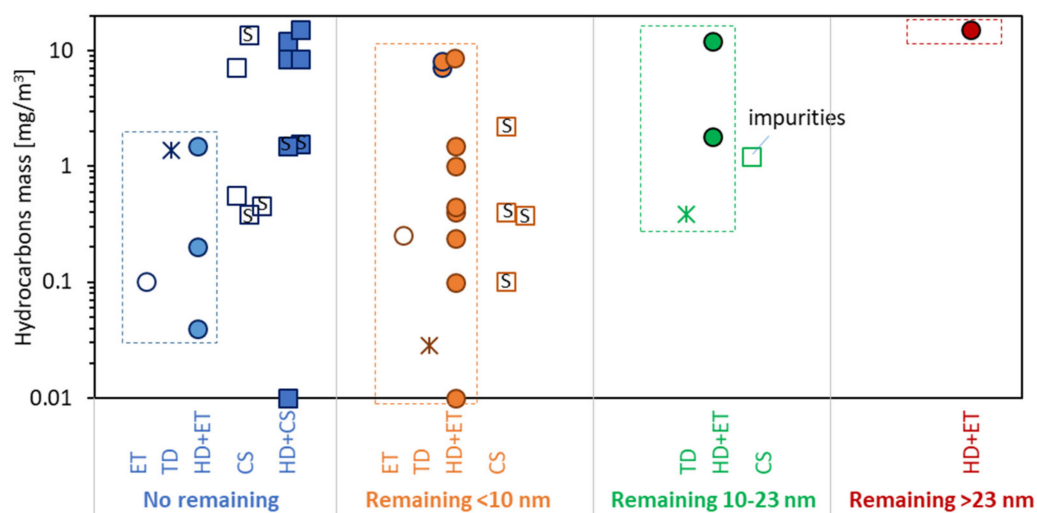


Figure 2. Volatile removal evaluation with hydrocarbons depending on whether none or some particles remained (or re-nucleated) <10 nm, between 10 and 23 nm, and >23 nm. Open circles: evaporation tubes (ET); asterisks: thermodenuders (TD); solid circles: hot dilution and evaporation tubes (HD + ET); open squares: catalytic strippers (CS); solid squares: hot dilution and catalytic strippers (HD + CS). “S” indicates CS with sulfur trap.

- No particles remained downstream of the system under evaluation (blue color). Note that typically the lower detection size of these studies was around 3–6 nm.
- Particles with sizes lower than 10 nm were detected downstream of the system under evaluation (orange color). These cases are of low risk for the future >10 nm regulation but could have artefacts with low cut-off counters.
- Particles in the size region 10–23 nm remained (green color). These cases are risky for the future >10 nm regulation and indicate hydrocarbons mass levels that could lead to “volatile” artefacts.
- Particles larger than 23 nm were detected (red color). These cases would affect also the results of the current >23 nm regulation.

In each area the results are separately plotted for:

- Standalone evaporation tubes (ET) (open circles).
- Thermodenuders (TD) (asterisks).
- Hot dilution (typically 10:1) plus evaporation tubes (HD + ET) (solid circles).
- Standalone catalytic strippers (CS) (open squares).
- Hot dilution plus catalytic strippers (HD + CS) (solid squares).

For better clarity the evaporation tube (stand alone or downstream of a hot dilution) and thermodenuder tests are enclosed in dashed squares. Only the tests with the maximum reported concentrations in each study are plotted.

The hot dilution plus evaporation tube (HD + ET) results resulted in artefacts >23 nm when challenged with 15 mg/m³ [34], while levels 2–12 mg/m³ had artefacts in the 10–23 nm range [36,39]. Artefacts <10 nm were detected with masses in a wide range of 0.01 mg/m³ to 8.5 mg/m³ [5,30,32,36,37,39–41]. On the other hand, no artefacts were seen with masses up to 1.5 mg/m³ for the combination of hot dilution and evaporation tube [43], confirming that the results might be system dependent. Standalone evaporation tubes (ET) could have artefacts <10 nm already at low levels (0.25 mg/m³) [5].

The catalytic stripper systems had no artefacts above 10 nm, with one exception which was probably solid residuals from impurities in the atomized material [45,48]. Masses up to 2 mg/m³ resulted in some particles remaining <10 nm for some standalone catalytic strippers [36,40,41,44]. For other standalone or with hot-dilution catalytic stripper systems, masses up to 8–15 mg/m³ had no particles remaining [34,36,39]. There was no difference between CS with or without sulfur trap, as both can remove hydrocarbon masses >10 mg/m³ without any remaining particles.

3.3. H₂SO₄

Figure 3 summarizes the results for H₂SO₄ and H₂SO₄ with hydrocarbons (C₂₄ or C₂₈) for evaporation tube-based [32,35,38–41] and catalytic stripper-based [32,35,38–41,44] systems. Particles >23 nm remained only with thermodenuder (3.8 mg/m³) [32] or evaporation tube after hot dilution (0.3 mg/m³) [39]. When the concentration was 1 mg/m³, some particles in the 10–23 nm range remained for the thermodenuder, and evaporation tube after hot dilution [40]. With mixture of H₂SO₄ with hydrocarbons, the evaporation tube had artefacts in the 10–23 nm range even at 0.1 mg/m³ [41]. Particles <10 nm remained even at very low masses (<0.2 mg/m³ of H₂SO₄ or H₂SO₄ and HCs) for the thermodenuder and the evaporation tube after hot dilution, although in one case, the evaporation tube with hot dilution could handle 2.5 mg/m³ with artefact <10 nm [38]. Only the catalytic stripper could completely remove sulfuric acid aerosol without any particle remaining at concentrations ranging from 0.1 mg/m³ [35,39,41] to 1 mg/m³ [38] or even 9.3 mg/m³ [44]. At the >10 mg/m³ range only one standalone catalytic stripper with a sulfur trap downstream of the oxidation catalyst was evaluated [44]. Although it could remove up to 9.3 mg/m³ H₂SO₄ without any particles remaining, at 16 mg/m³ some particles remained below 10 nm, and at 28 mg/m³ particles remained at the 10–23 nm range. Only one study compared a catalytic stripper with and without a sulfur trap [40]. The version with sulfur trap could handle up to 1 mg/m³ without significant artefacts while without the trap remaining particles were detected already on H₂SO₄ concentrations above 0.07 mg/m³. In general, catalytic strippers with a sulfur trap could handle higher H₂SO₄ containing aerosol.

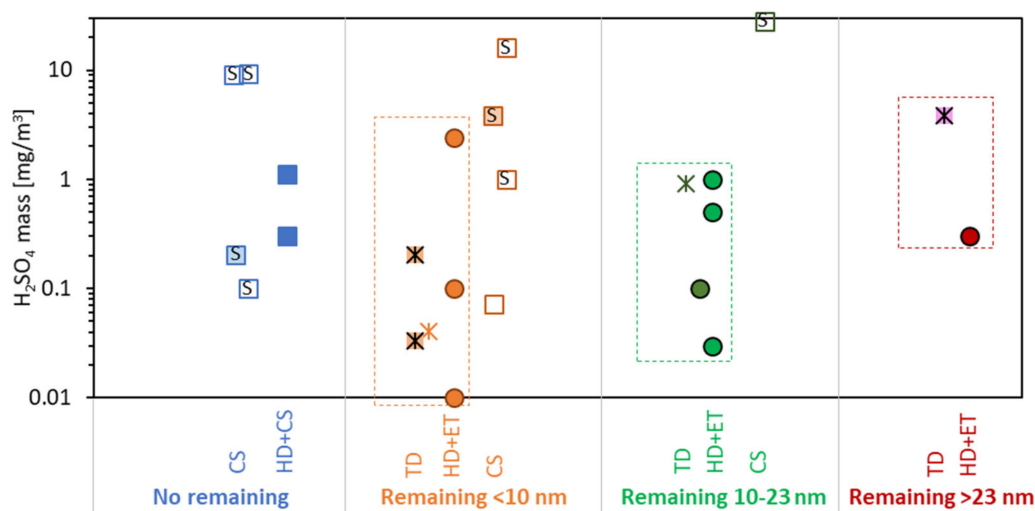


Figure 3. Volatile removal evaluation with sulfuric acid aerosol or sulfuric acid and hydrocarbons (symbols with background) depending on whether none or some particles remained (or re-nucleated) <10 nm, between 10 and 23 nm, and >23 nm. Open circles: evaporation tubes (ET); asterisks: thermodenuders (TD); solid circles: hot dilution and evaporation tubes (HD + ET); open squares: catalytic strippers (CS); solid squares: hot dilution and catalytic strippers (HD + CS). “S” indicates CS with sulfur trap.

3.4. Ammonium Sulfate

A catalytic stripper based on a commercial vehicle aftertreatment DOC, used downstream of a hot dilution, could evaporate and shrink ammonium sulfate particles, but a residual with a mean between 10 nm and 20 nm remained due to the atomization method [29]. In another study, a CS downstream of a hot diluter started to show some breakthrough only at inlet concentration of around 1×10^7 p/cm³ (8.5 mg/m³) [39]. The hot diluter and evaporation tube combination had breakthrough at a one order of magnitude lower concentrations. A later study confirmed the findings and showed that the breakthrough particles had a size <23 nm [38].

3.5. Vehicles' Exhaust

Figure 4, which is organized in the same way as the previous figures, summarizes the results with vehicles' exhaust for evaporation tube [3,8,33,34,41,49–57] and catalytic stripper [3,8,33,34,41,50,52,57] systems. The volatile mass concentrations refer to the inlet of the systems, which were sampling from the full dilution tunnel. They were estimated from the nucleation mode size distributions. The horizontal lines indicate the levels of volatiles of the different tested categories: mopeds >10 mg/m³, diesel with DPF but without diesel oxidation catalyst (DOC) 6 mg/m³, and all the rest (GDI, DPF regenerations and heavy duty diesel vehicles) <1 mg/m³. The chemical composition of the volatiles is unknown (i.e., was not measured in any of the studies).

The hot dilution and evaporation tube had cases with remaining particles even at low levels: with 0.05 mg/m³ there were particles <10 nm [41], while with mass 0.5 mg/m³ or higher particles 10–23 nm remained (in one case also particles >23 nm) [49]. However, there was a case in which the hot dilution and evaporation tube could handle 15 mg/m³ without artefacts (primary hot dilution 25:1) [34]. The catalytic stripper (standalone or downstream of a hot dilution) did not have cases where particles >10 nm remained. There were cases that particles <10 nm remained at mass concentrations 0.65 mg/m³ [52] or 6.1 mg/m³ [33] (as standalone) or 30–50 mg/m³ downstream of a hot dilution [8,34]. There were many experiments with CS that no particles remained with concentrations even >10 mg/m³.

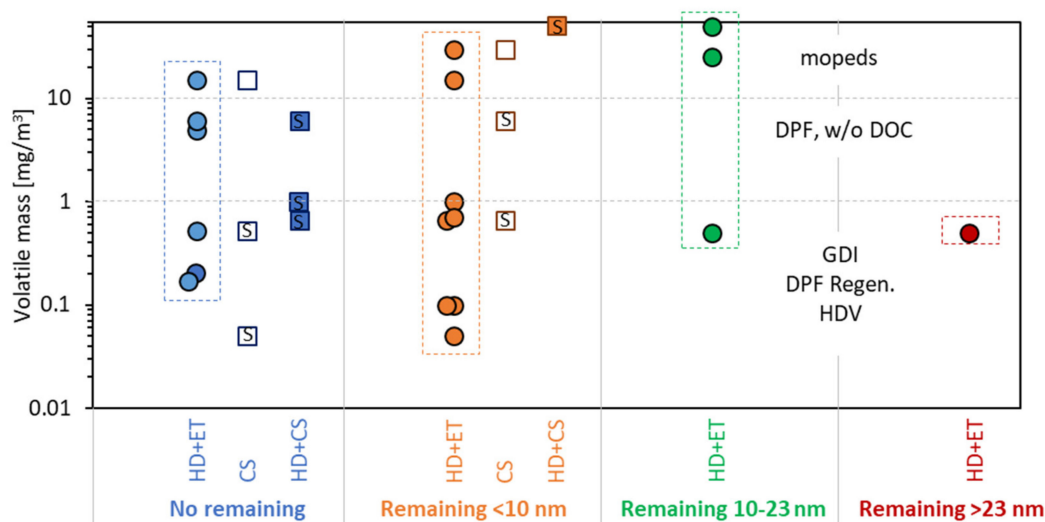


Figure 4. Volatile removal evaluation with vehicles' exhaust depending on whether none or some particles remained (or re-nucleated) <10 nm, between 10 and 23 nm, and >23 nm. Solid circles: hot dilution and evaporation tubes (HD + ET); open squares: catalytic strippers (CS); solid squares: hot dilution and catalytic strippers (HD + CS). "S" indicates CS with sulfur trap. DOC = diesel oxidation catalyst; DPF = diesel particulate filter; GDI = gasoline direct injection; HDV = heavy-duty vehicle.

4. Discussion

This review summarized the studies that evaluated evaporation tubes and catalytic strippers with laboratory or vehicles' exhaust aerosol. The implications of the results will be discussed in the following sections.

4.1. Evaporation Tube

The concept that was introduced in the particle number regulations is very efficient, as summarized in the literature [14]. The hot dilution with the evaporation tube in combination with a counter that measures particles >23 nm is a reliable methodology as artefacts have rarely been reported.

The temperature of the evaporation tube and the residence time is appropriate for the evaporation of volatile particles. The theory estimates necessary time around 10–16 ms for typical commercial systems [5,44], which is much less than the 200–400 ms residence time in the systems, although the available time at the critical temperature region (>250 °C) is shorter. The upstream dilution at 150 °C pre-heats the sample and ensures that the desired temperature will be reached in the evaporation tube. Most importantly, it dilutes the sample and reduces the partial pressures, thus minimizing the possibility of nucleation downstream of the evaporation tube. Nevertheless, nucleation has been reported many times with both laboratory and vehicles' exhaust aerosol. Theoretically, the nucleation of hydrocarbons is unlikely because very high concentrations are required (>3 mg/m³ [5]). However, the experimental data with laboratory hydrocarbon aerosols showed that standalone evaporation tubes could not handle 0.25 mg/m³. Evaporation tubes, even with a hot dilution upstream (dilution 10:1), could not handle 8.5 mg/m³ (0.85 mg/m³ at the inlet of the evaporation tube) as particles <10 nm remained (or nucleated). The case where particles >23 nm remained was atomized emery oil (15 mg/m³) with hot dilution 25:1. In this case it is possible that there were impurities and the evaporated emery oil condensed on the solid residuals downstream of the evaporation tube growing them to the over 23 nm range [48].

When sulfuric acid is available, formation of nucleation particles is very probable. Theoretical calculation and experimental results have shown nucleation possibility even at 0.3 µg/m³ levels [5]. Small amounts of ammonia (<20 ppb) may significantly enhance the binary nucleation rate of sulfuric acid and water [58–60], for example at vehicles with SCR (selective catalytic reduction for NO_x)

systems or gasoline vehicles with three-way catalysts (TWC) [61]. Experimentally, nucleation particles downstream of a VPR with evaporation tube were measured from a heavy-duty vehicle equipped with SCR [62]. However, the size of the H_2SO_4 nuclei (critical clusters) is approximately 1–1.5 nm and high concentrations of H_2SO_4 are needed to grow them to 3 nm in diameter [63,64]. Interestingly, laboratory experiments with sulfuric acid (and humidity) have reported size distributions peaking at 18 nm [65] or even >200 nm [44]. Similarly, experiments with SO_2 (converted to SO_3) gave nucleation modes peaking at 16 nm (1.8 ppm SO_2) [66], 45 nm (61.4 ppm SO_2) [66], or even >70 nm (200 ppm) [33].

Nuclei typically grow to bigger than 3 nm sizes with organics [67], even at low concentrations as experiments with heavy-duty engine have shown [68]. The fuel sulfur was 1 ppm, and the (effective) contribution of the lubricant was 2–9 ppm (estimated sulfuric acid concentration $1.5\text{--}5.8 \times 10^{12} \text{ cm}^{-3}$) and the final mean size was <10 nm [69]. The nucleation mode peaked at 15 nm when the sulfur (fuel plus effective lubricant) was approximately 50 ppm (sulfuric acid $3.3 \times 10^{13} \text{ cm}^{-3}$). Growth rates of 6–24 nm/s were measured for a heavy-duty engine with 8 mg/m^3 organics emissions [70]. Another study found a nucleation mode of 6 nm when organics were available with concentration 10^{11} cm^{-3} [71]. With appropriate residence time (1 s), in the presence of a high amount of organics (10^{14} cm^{-3}) the nucleation mode peaked at 20 nm [72]. Approximately 1 ppm of propane corresponds to $1 \times 10^{12} \text{ cm}^{-3}$ organics [73]. This is calculated using the appropriate molecular mass and an assumed 10–30% fraction of total organics potentially condensing on the particulates phase [73]. Thus, it can be assumed that with hydrocarbon concentrations >100 ppm at the outlet of the evaporation tube the nucleated sulfuric acid particles can grow to sizes of 20 nm.

The laboratory tests with sulfuric acid (and hydrocarbons in some cases) confirmed the previous studies. In all cases with the evaporation tubes there was re-nucleation. Mass of 0.9 mg/m^3 or lower resulted in nucleation mode particles >10 nm even with a hot dilution of 10:1. However, for the majority of the cases, with high dilution ratios (>100:1 primary hot dilution) there are no reported cases of re-nucleation [74] except with 2-stroke mopeds. Studies comparing evaporation tubes with catalytic strippers gave equivalent results (within 10%) for both 23 nm and 10 nm systems [39,75,76]. Higher differences of the 10 nm systems were attributed to the different cut-off curves of the counters.

4.2. Catalytic Stripper

The studies with catalytic strippers proved that much higher concentrations can be handled for both hydrocarbons and/or sulfuric acid aerosols than with evaporation tubes. For example, no artefacts were seen when catalytic strippers were challenged with hydrocarbons. In a few cases without hot pre-diluter particles <10 nm remained. Similarly, most concentrations of sulfuric acid were efficiently removed. Only in a few cases standalone systems had particles remaining <10 nm. The results with vehicle exhaust were similar to the laboratory aerosols. The standalone catalytic stripper had in some cases particles remaining <10 nm, while the evaporation tube systems often had particles remaining >10 nm at various challenge mass levels.

The conclusion based on the current experimental results is to use a catalytic stripper when measurements of particles >10 nm are conducted. For lower sizes, the catalytic stripper is necessary, but not artefact-free, and a hot pre-diluter is recommended. For lower than 10 nm measurements, the high particle losses of the catalytic stripper have also to be considered.

4.2.1. Oxidation and Sulfur Trap Parts

Figure 5a plots separately examples of the two parts of a catalytic stripper: the oxidation part and the sulfur storage part. In actual catalytic strippers the two parts are continuous. At some catalytic strippers the sulfur trap is upstream of the oxidation part, in some downstream, and in some others it does not exist. As discussed before (Figure 1), the oxidation part evaporates nucleation mode particles and oxidizes the volatile particles (actually the particles should be evaporated earlier in an evaporation tube in order to have more efficient oxidation in the gaseous phase). The condensed material on the soot particles is also evaporated and oxidized. In this oxidation part the SO_2 and SO_3

are considered to remain unaffected; especially catalytic strippers without a sulfur trap rely on this assumption. The actual SO_2 to SO_3 conversion, however, depends on the catalyst formulation as will be discussed in Section 4.2.2. Modern engines equipped with oxidation converters and depending on the fuel and lubricant sulfur content, can have relatively high SO_3 concentrations and this could result in nucleation of sulfuric acid at the exit of the catalytic stripper. The sulfur trap retains sulfur, minimizing this possibility.

At low temperatures ($<350\text{ }^\circ\text{C}$) sulfur is stored through adsorption or condensation (physically bounded sulfate), while, at higher temperatures ($>400\text{ }^\circ\text{C}$) sulfur is stored as chemically bound metal sulfate [77]. Adhesion of sulfate in mist form on the catalyst is also possible at low temperatures. Under oxygen deficient conditions H_2S is formed, which is poisonous for metal surfaces.

Sulfur traps may include an oxidation catalyst, e.g., platinum, to facilitate the SO_2 to SO_3 reaction. Typical sulfur storage systems are based on alkaline earth or alkali metal oxides and their mixtures on alumina washcoat. Other materials such as zinc, nickel, chromium, and copper are used either as stand-alone scavengers or as promoters, to modify trap performance, strengthen desired reactions, and influence the adsorption/desorption temperatures.

4.2.2. SO_2 to SO_3 Conversion

Figure 5b summarizes SO_2 to SO_3 conversion efficiencies from the literature of commonly used oxidation catalysts (based also on the review in [78]). The space velocity was around $35,000\text{--}50,000\text{ h}^{-1}$. Higher space velocities result in lower conversions [79,80]. Conversion rates for other catalyst materials can be found in the literature (e.g., [81,82]). The extent of the conversion depends mainly on the exhaust gas temperature, the type of noble metal used and the loading, and composition of the washcoat. The SO_2 to SO_3 conversion starts to increase at around $200\text{ }^\circ\text{C}$, reaches a maximum at $450\text{ }^\circ\text{C}$ as the reaction kinetics accelerate and then gradually decreases due to thermodynamic equilibrium limitations. The three studies with catalytic strippers are in agreement with the published data and vary from 0% to 37.5% at $275\text{ }^\circ\text{C}$ to $300\text{ }^\circ\text{C}$ actual aerosol temperature [30,33,36]. The need for a low or high SO_2 to SO_3 conversion depends on the concept of the catalytic stripper (only oxidation part or with sulfur trap).

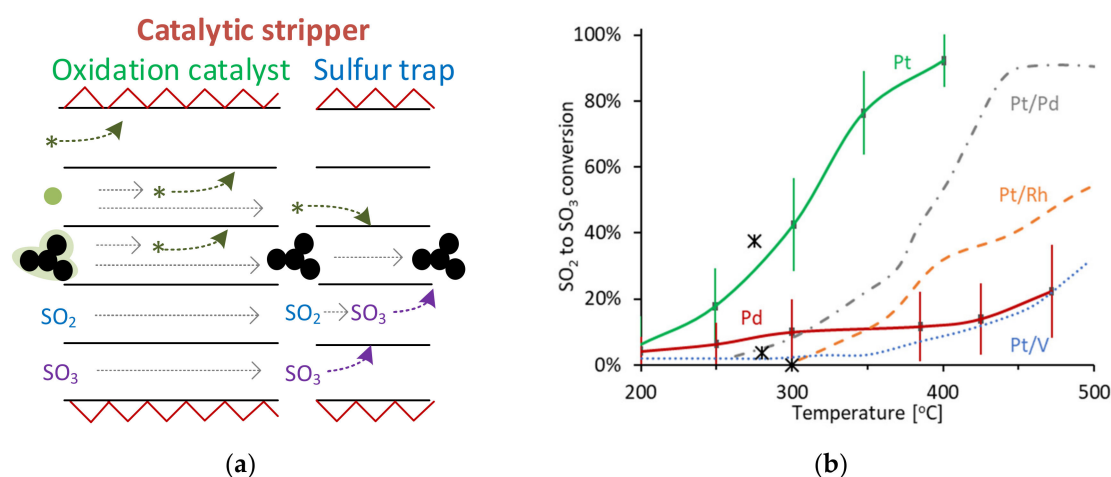


Figure 5. Catalytic stripper: (a) the two parts of a catalytic stripper: oxidation catalyst and sulfur trap. Products of reactions such as CO_2 and H_2O are not plotted; (b) SO_2 to SO_3 conversion for various noble metals and combinations. Pt [79,83–86], Pt/Pd [87], Pt/Rh [87], Pt/V [84], Pd [84,87]. Asterisks are experimental data with catalytic strippers [30,33,36].

4.2.3. Storage Capacity

The SO_x (SO_2 and/or SO_3) retention capacity is typically expressed in milligrams of SO_x captured per gram of sorbent. A review of the literature of sorbent systems for the removal of the SO_x from

flue gases reported values from a few mg to hundreds of mg per gram of sorbent [88]. In vehicle applications, the catalyst capacity in sulfate storage depends on the noble metal and the washcoat composition. Studies with diesel oxidation catalysts (DOCs) with 1% Pt on alumina found 16–50 mg sulfates per gram of washcoat (1.6–5%) at 350 °C [80,89,90], but 0% for SiC washcoat [89]. A Pd on alumina adsorbed up to 7% SO₂ at 320 °C [91]. At temperatures higher than 400 °C, percentages of up to 4% have been reported for Pt, Pt/Pd, or Pt/V catalysts [84,92–94]. Dedicated studies with sulfur traps have reported SO₂ capacity of 40–70% at temperatures 300–400 °C [95,96].

Materials are generally post-characterized for total sulfur content. However, a substantial concentration of SO₃ can be present in the flue gas well before the total capacity is reached [81]. This means that the total capacity of an absorber or adsorber is a poor indication of actual performance during operation. Therefore, the performance of catalytic strippers is characterized in real time.

Figure 6 plots a hypothetical sulfur storage test based on published similar studies [20,33,36,83,97–103]. At time t_0 , SO₂ in O₂ and N₂ is inserted in the catalytic stripper. The SO₂ level is typically between 20 and 150 ppm (100% in the figure) in order to have adequate measurement accuracy with the SO₂ analyzer. Initially, the measured SO₂ outlet concentration is zero because the SO₂ is stored in the trap (either as SO₂ or metal sulfate after conversion to SO₃). At some point (t_b) breakthrough of SO₂ will start. From this point, the trapping efficiency is not 100%. SO₃ will also start to appear at the outlet of the catalytic stripper. For simplification, in this figure, it is assumed that SO₃ appears at the same time with the SO₂, but this is not necessarily true. This SO₃ poses a risk for particles formation. Figure 6b gives an example of a particle size distribution measured at the outlet of the catalytic stripper during the breakthrough period (t_2). Note that during the initial storage phase no particles were emitted (t_1). At point (t_{eq}) the sulfur storage capacity will be saturated and the SO₂ and SO₃ outlet concentrations will be stabilized. From t_{eq} the sulfur trap is behaving like an oxidation catalyst and produces SO₃ with high probability for particle formation (Figure 6b, size distribution t_3). The exact time of appearance and the magnitude of the size distributions depend on many parameters such as SO₂ levels, SO₂ to SO₃ conversion rate, humidity, and availability of hydrocarbons [33,66]. The transition from t_b to t_{eq} was plotted as a linear function for simplicity reasons; however, in reality it is sigmoidal-like curve.

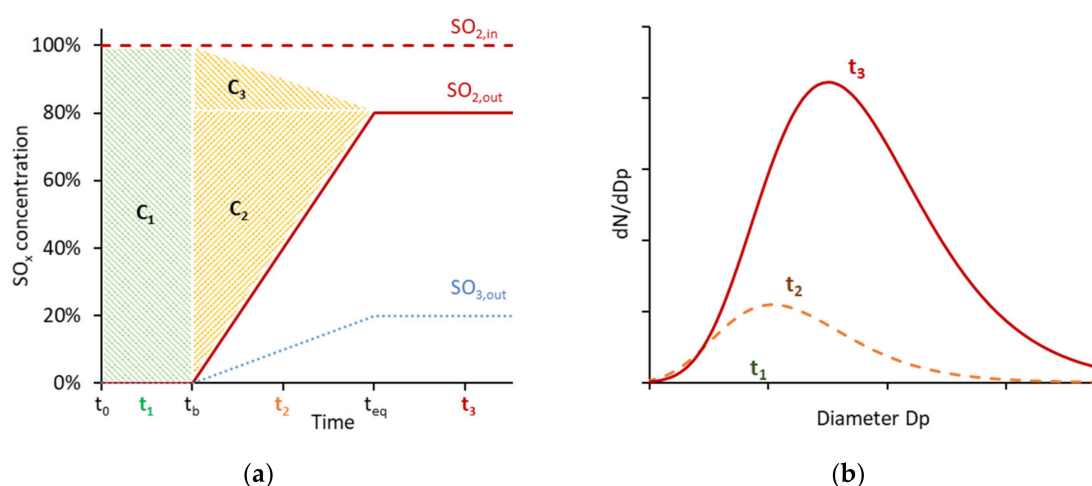


Figure 6. Hypothetical sulfur storage test with SO₂: (a) SO_x concentrations over time; (b) particle size distributions during the sulfur storage test.

The “total storage capacity” area is $C_1 + C_2 + C_3$. Note that usually there are no SO₃ measurements, so the determination of C_3 is not possible and not reported. Note also that even if the SO₃ breakthrough starts after the SO₂ breakthrough, the definitions of the areas remain the same, because if there is already SO₃ in the aerosol, it might not be completely stored in the sulfur trap already at time t_b . The important area, however, is C_1 , which is called “complete storage capacity”. The determination of

the breakthrough point (t_b) is typically set to 1% SO₂ to cover the uncertainty of the SO₂ measurement, but 0% has also been used for catalytic strippers.

The sulfur mass C_m [mg/s] passing through the catalyst is:

$$C_m = 10^{-6} \times C_v \times \rho_{SO_2} \times (Q/60) \times (M_S/M_{SO_2}) \times 10^3, \quad (1)$$

where C_v is the SO₂ passing through the catalyst [ppmv], ρ_{SO_2} is the density of SO₂ at 0 °C [2.86 g/L], Q is the catalytic stripper flow rate at 0 °C [L/min], M_S is the molecular mass of sulfur [32 g/mol], M_{SO_2} is the molecular weight of sulfur dioxide [64 g/mol]. The sulfur capacity C [mg S] can be estimated by integrating C_m for the appropriate time and assuming a retention efficiency R . Typically, the “complete” capacity should be reported (C_1 in Figure 6a), where the retention efficiency R is 100% (integration until t_b). After t_b the retention efficiency can be estimated from the surface area of the graph.

$$C = \sum_{0-t} (R_i \times C_m). \quad (2)$$

The composition and the amount of the washcoat of catalytic strippers is not disclosed, so “total” captured sulfur mass is reported (or mass/L of catalyst). Values of approximately 6–23 mg or 0.7–1 g/L have been reported [33,36], with re-nucleation artefacts beginning already at 20–40% of the capacity. It can be assumed that research in this area can further increase the storage capacity. For example, a sulfur trap stored almost up to 15 g/L with no evidence of poisoning of a NO_x catalyst downstream of the sulfur trap [104].

Based on Equations (1) and (2), the time until saturation t [h] of a catalytic stripper with sulfur trap can be estimated based on the following equation:

$$t = 11.7 \times C/Q/E, \quad (3)$$

where E are the expected SO_x emissions [ppmv SO_x]. Assuming 2.5 mg effective (complete) sulfur capacity (C_1 in Figure 6a) and 1 L/min flowrate, for 0.5 ppm SO_x emissions, the time until saturation would be 58 h. Considering the dilution at the dilution tunnel and at the pre-diluter, this time would increase approximately 100 times. Similarly, a system at the tailpipe would also use a high dilution of at least 100:1. It should be highlighted that a catalytic stripper used directly at the tailpipe needs some dilution in order to ensure that enough oxygen will be available for oxidation at rich or stoichiometric modes of engine operation.

4.2.4. Position of Sulfur Trap

The first CS with sulfur trap had the trap upstream of the oxidation catalyst in order to protect the oxidation catalyst from poisoning [31,105], because the sulfates formed inhibit reactants from adsorbing on the active sites [77,106]. Tests showed that the total sulfur capacity was 60% lower compared to the configuration where the sulfur trap was downstream [33]. It was assumed that, the sulfur was primarily stored as SO₂, because no SO₃ was available upstream of the sulfur trap. Further tests showed that poisoning of the oxidation catalyst (saturated with sulfur) did not affect the volatile removal [36]. Nevertheless, the light-off temperatures were lower when the sulfur trap was upstream [33]. As the catalytic stripper is used at a constant high temperature (350 °C), the light-off temperature is not of concern. For these reasons, the downstream position is the preferred one in commercial systems.

4.3. Open Issues

The superiority of the catalytic stripper compared to the evaporation tube for sub-23 nm measurements was shown experimentally in many studies. The addition of a sulfur trap in many cases gave an advantage of retention of sulfuric acid. However, there are no technical requirements or specifications for catalytic strippers, so non-optimized systems might be used resulting in lower

than expected performance. The following sections will discuss issues related to particle losses, sulfur storage capacity, and typical vehicles' aerosol.

4.3.1. Particle Losses

The particle losses in a volatile particle remover are due to diffusion and thermophoresis. The thermophoretic losses are around 25% without any dilution downstream of the volatile particle remover, but less than 10% with dilution. The diffusion losses are size-dependent and for catalytic strippers are from 15% to 40% more compared to 100 nm [29,33,36]. The thermophoretic losses are similar for catalytic strippers and evaporation tubes for similar setup. The major drawback of catalytic strippers versus evaporation tubes is the additional size dependent diffusion losses. Tests with a particle number system replacing the evaporation tube with a catalytic stripper gave <20% difference at the 10 nm losses [39]. The design of a catalytic stripper is a compromise between volatile removal efficiency and non-volatile particles' penetrations [29,44]. Particle number systems with optimized catalytic strippers have achieved <20% losses at 10 nm [29,36], but typically the losses are higher [39,107]. The regulation uses an average particle number concentration reduction factor (PCRF) of 30 nm, 50 nm, and 100 nm to take into account the particle losses and the dilution ratio. This average PCRF is based on the fact that vehicles' size distributions have geometric mean diameter around 50 nm. In order to minimize the influence of the small particle losses on the results, restrictions for the sub-23 nm sizes are necessary. The future >10 nm regulation will have a limit for the ratio $PCRF_{15}$ to $PCRF_{100}$ of <2. Another solution is to use two particle number counters with different cut-off sizes (at 23 and 10 nm, approximately) and correct for the losses below 23 nm [8].

For 30 nm (and larger) sizes the differences of the losses between identical systems with evaporation tubes or catalytic strippers are less than 10% [39]. This value is well within the range seen between various commercial systems with evaporation tubes. The average PCRF, which takes into account the losses at 30 nm, 50 nm and 100 nm, will partly offset the size-dependent losses. Furthermore, the penetration of the complete system does not depend so much on the VPR, but mainly on the PNC [76]. Consequently, the differences of the systems with 23 nm PNCs will be within the typical experimental uncertainties (5%). Indeed, most comparisons of >23 nm systems with and without catalytic strippers gave comparable results [39,75,76]. With the current regulations, catalytic strippers are not allowed in the volatile particle removers, because it is required that the materials do not react with exhaust gas components. However, assuming that a system with catalytic stripper fulfils all the rest requirements (e.g., $PCRF_{30}$ to $PCRF_{100}$ ratio <1.3), and based on the aforementioned findings, there is no reason to exclude catalytic strippers for >23 nm measurements. Thus, future regulation should permit the use of catalytic strippers even for measurements of particles >23 nm.

4.3.2. SO₃ Conversion Risks

The catalytic strippers with only the oxidation part do not convert SO₂ to SO₃, but this needs to be checked, because at the temperature required by the regulation (350 °C) some conversion may take place (as discussed in Figure 5b). This could result in higher risk for re-nucleation compared to an evaporation tube (where no SO₂ to SO₃ conversion takes place). In this case it is necessary that most of the hydrocarbons are removed, so the nuclei will not grow to the measurement range of the counting instruments.

Catalytic strippers with sulfur trap showed efficient removal even for high concentrations of sulfuric acid. However, the risk with these systems is that they may be saturated if proper attention is not given. At the moment there is no alarm/warning for such cases. Due to their high SO₂ to SO₃ conversion, when they are saturated they may result in higher nucleation probability compared to the simple oxidation catalytic strippers or evaporation tubes. For modern light-duty vehicles with low sulfur fuel and lubricant, the time until saturation is hundreds of hours (with some dilution) [33]. For applications using high sulfur content fuels (e.g., marine engines), however, they could saturate only in a couple of hours [35]. Maximum SO₂ concentrations are given in Table 2 for recent technologies (and

fuels). Higher concentrations could be measured when the fuel sulfur content is >15 ppm, e.g., in India, Central and South America or in Africa [108]. For example, the expected SO₂ concentrations are <1 ppm for modern vehicles [35], and peaks of 20 ppm may appear, and in extreme cases (e.g., regenerations) even higher (150 ppm) [109]. However, measurement campaigns in countries with high sulfur content fuel have reported average SO₂ concentrations of 20–120 ppm [110] or even higher when there were maintenance issues with the vehicles [111]. As it was discussed in Figure 6b, high SO₂ or SO₃ concentrations can result in sulfuric acid nucleation particles peaking at sizes >10 nm [33,66].

In addition to the SO₂ to SO₃ reaction, it is not well understood how the catalytic strippers react with the exhaust aerosol. In a few cases non-volatile particle formation has been found in evaporation tubes, but also in catalytic strippers [32,41]. In another case, a catalytic stripper measured higher non-volatile particle concentrations than an evaporation tube [50]. This is an area that needs further research.

4.3.3. Vehicles' Volatile Aerosol

Table 2 gives the mass of volatiles reported as nucleation mode (NM) particles in the literature. These are the actual (maximum) levels that particle number systems may be challenged with. What is not always known is the chemical composition, and when detailed analysis is undertaken, hundreds of compounds can be found [112]. Furthermore, it is not possible to define easily a “typical” composition as it depends on the engine out emissions, the aftertreatment devices, the fuel, the lubricant, and the driving style. For example, for a heavy-duty engine without aftertreatment devices, branched alkanes and alkyl-substituted cycloalkanes from unburned fuel and/or lubricating oil contributed >95% of the nanoparticle mass, and sulfuric acid <5% [113]. Another study indicated that the organic component of diesel nanoparticles comprised compounds with carbon numbers in the C₂₄–C₃₂ range, derived almost entirely from unburned oil [114]. For a heavy-duty diesel vehicle with a catalyzed continuously regenerating trap (CRT) and 420 ppm sulfur fuel the majority of the NM was sulfates [115]. Similarly, for light-duty NM particles, the sulfate to organic ratios were from 0.2 to 20 depending on the engine load (and exhaust gas temperature) for 350 ppm fuel sulfur [116]. Chemical analysis of a heavy-duty DPF having mainly nucleation mode particles (1.2×10^{11} p/km) showed a high amount of BTEX compounds (benzene, toluene, ethylbenzene, m,p-xylenes, and o-xylene) and PAHs (polycyclic aromatic hydrocarbons) [117]. Similar results were noted for light-duty vehicles and, additionally, alkanes had high concentrations [118]. Toluene, isopentane, m,p-xylene, 1,2,4-trimethylbenzene, and o-xylene were the dominant volatile organic compounds emitted from the tailpipe exhaust of the motorcycles [119].

Table 2. Peak concentrations during cold start, during the test cycle or regenerations. HCs and SO₂ concentrations refer to the tailpipe, NM to the dilution tunnel. HC = hydrocarbons; HD = heavy-duty; LD = light-duty; NM = nucleation mode.

Technology	Period	NM [mg/m ³]	Gas HCs [ppm]	SO ₂ [ppm]	References
Moped	Cold start	>10	>50,000	60	[8,34,49]
Motorcycle	Cold start		10,000–35,000	12–20	[120–122]
Motorcycle	Cycle	0.4	300–5000	9–20	[123,124]
LD Gasoline	Cold start	5	12,000	10	[125–130]
LD Diesel	Cold start	low	350	10	[128,131]
LD Diesel	Regeneration	1	200	25	[57,132–134]
HD Diesel	Regeneration	1–12	250	150	[109,115,135–139]

For completeness, examples of measured gaseous hydrocarbons are given in Table 1. They are measured according to the regulated procedure (with heated line at 191 °C), thus they represent “light” hydrocarbons and they do not necessarily correlate with the NM reported in the same table. Furthermore, typically less than 30% of total HC is condensed on soot particles. The catalytic strippers remove the hydrocarbons more efficiently in the gas phase than in the particle phase [33]. Thus, the

interpretation of these concentrations as requirements for catalytic strippers should be done with precaution. Moreover, the gas oxidation efficiency check may not be necessary if the volatile particles' removal efficiency is checked. Nevertheless, it could be a useful and easy check for the long term volatile removal efficiency stability, especially as the catalytic stripper is poisoned by sulfur compounds over time. At the temperatures prescribed in the regulations (300–400 °C) the oxidation efficiency of CH₄ is low, thus a gas such as propane is more suitable and also typically available in most laboratories that do vehicle emissions testing (for calibration of other gas analyzers).

4.3.4. Catalytic Stripper Technical Requirements

Table 3 gives suggestions for future tests that could be required for the characterization of catalytic strippers (standalone or in a VPR system). Examples and citations where more details can be found are also given. Regarding particle losses, the requirements of the regulation should be fulfilled, i.e., PCRF₁₅ to PCRF₁₀₀ ratio <2. The wall temperature is also defined in the requirements, usually between 300 °C to 400 °C. For catalytic strippers, it seems that the lower temperature limit is more advantageous because the SO₂ to SO₃ conversion is lower. This conversion ratio should be reported, especially for systems without a sulfur trap, which should have very low conversion. Systems with a sulfur trap should report the sulfur storage capacity. Two values should be reported: the complete (i.e., until no SO₂ is measured downstream of the catalytic stripper) and the total (i.e., until the SO₂ concentration at the outlet of the catalytic stripper is stabilized). The measurement of SO₃ (and H₂SO₄) is challenging. In the presence of water vapor in particular, sulfuric acid will be formed, that is corrosive and there are concerns regarding potential damage to the analytical equipment or even artefacts [81]. The particle removal efficiency should also be given. At the moment the preferred generation method is evaporation-condensation technique with tetracontane particles, as the atomization method of oils can result in residual particles from impurities in the atomized material. Even though the oxidation efficiency (e.g., of propane) is not so relevant for the specific application of catalytic strippers, it could be evaluated as a simple check of the long-term stability of the oxidation efficiency.

Table 3. Suggestions for technical requirements of catalytic strippers. The references give the experimental setups of the proposed tests. HC = hydrocarbons; VRE = volatile removal efficiency.

Test	Comment	Example	Reference
Particle losses	As required in the regulation		[33,36]
Wall temperature	As required in the regulation	300 °C to 350 °C	Regulation
SO ₂ to SO ₃ conversion	To be declared	%	[33,36]
Sulfur storage capacity	Based on SO ₂	mg	[33,36]
VRE H ₂ SO ₄	Feasibility to be assessed	>99.9%; >1 mg/m ³	[39,44]
VRE gaseous HCs	Long term efficiency C ₃ H ₈	>99.9%; >10,000 ppm	[33]
VRE particle HCs	Tetracontane particles	>99.9%; >1 mg/m ³	[30,33,36]

5. Conclusions

This review summarized the volatile removal efficiency of evaporation tubes (ET), thermodenuders (TD), and catalytic strippers (CS). Some of the catalytic strippers had only an oxidation part and some had, additionally, a sulfur trap upstream or downstream of the oxidation part.

Theoretically, CS oxidize the hydrocarbons resulting in smaller (if any) growth of any volatile nucleation mode particles, compared to evaporation tubes that reduce hydrocarbons only by dilution. CS with sulfur traps store sulfur compounds, thus, further minimizing any possibility of nucleating particles. On the other hand, if the sulfur trap is saturated, any existing SO₃ or SO₃ formed in the CS might enhance nucleation. At very high SO₂ and/or SO₃ concentrations the nucleated particles may grow to the measuring range of the instruments. Considering that modern vehicles emit some SO₃ (and thus there is potential for nucleation) and the ET does not oxidize the hydrocarbons, the

CS is a safer option for avoiding volatile artefacts (i.e., measuring re-nucleated volatile particles as non-volatiles).

The summary of the published experimental results showed that ET and TD could handle up to 2 mg/m³ of hydrocarbons without artefacts, but in some cases particles <10 nm remained. Masses >2 mg/m³ resulted in artefacts in the 10–23 nm range or even >23 nm (15 mg/m³) on some occasions. CS did not have any artefacts >10 nm in any of the studies (with one exception that were presumably solid residuals). Inlet masses up to 13 g/m³ could be handled with CS in most cases without any particles remaining, but in some cases particles <10 nm were detected after CS even at hydrocarbon compound masses below 2 mg/m³.

With sulfuric acid containing aerosol, particles were always detected downstream of ET and TD: they were <10 nm with <0.2 mg/m³ upstream concentrations (with one exception of hot dilution and evaporation tube that could handle up to 2.5 mg/m³). The CS could efficiently handle the sulfuric acid aerosol. However, at concentrations >1 mg/m³ some particles below 10 nm remained. The limited data show that with a sulfur trap higher masses can be handled. In two cases, CS with a sulfur trap could handle at least 9 mg/m³ without any particles remaining.

The vehicle exhaust aerosol had remaining particles larger than 10 nm for masses >0.5 mg/m³ and <10 nm even for masses of 0.05 mg/m³ for the ET systems. The CS had no cases with remaining particles >10 nm. There were cases with particles <10 nm when the mass was 0.65 mg/m³ (standalone) or 50 mg/m³ (downstream of hot dilution).

In general, the experimental results of the reviewed studies showed that the CS is the safest option for minimum artefacts for measurements >10 nm. Studies below 10 nm still need attention, even with CS, both regarding the volatile removal efficiency, but also the high particle losses. The above results also confirm that the CS should be allowed in place or in addition to the ET of the existing systems measuring >23 nm.

Due to the substantial variability of the results and the different removal efficiencies of the various systems, in order to standardize the evaluation of the systems, it is recommended to include a volatile removal efficiency test. Realistic levels of challenge aerosol should be in the order of 1 mg/m³ (except mopeds that exceed 10 mg/m³). At the moment, it is not clear what is a representative chemical composition of the volatile particles, but it seems that sulfuric acid plays a major role in their formation and should also be included in the volatile removal assessment of the systems. However, H₂SO₄ is corrosive and there are concerns regarding potential damage to the analytical equipment or even artefacts. Catalytic strippers with sulfur traps should report their storage capacity and those without, should confirm that no (or minimum) SO₂ to SO₃ conversion takes place.

Author Contributions: Conceptualization, B.G.; formal analysis, B.G.; writing—original draft preparation, B.G. and A.D.M.; writing—review and editing, T.L. and G.M.; All authors have read and agreed to the published version of the manuscript.

Funding: This research received no external funding.

Acknowledgments: The authors would like to acknowledge the comments of A. Mamakos and Y. Otsuki at earlier draft versions. B.G. appreciates the discussions with L. Ntziachristos.

Conflicts of Interest: The authors declare no conflict of interest.

References

1. Giechaskiel, B.; Maricq, M.; Ntziachristos, L.; Dardiotis, C.; Wang, X.; Axmann, H.; Bergmann, A.; Schindler, W. Review of motor vehicle particulate emissions sampling and measurement: From smoke and filter mass to particle number. *J. Aerosol Sci.* **2014**, *67*, 48–86. [[CrossRef](#)]
2. Giechaskiel, B.; Mamakos, A.; Andersson, J.; Dilara, P.; Martini, G.; Schindler, W.; Bergmann, A. Measurement of automotive nonvolatile particle number emissions within the European legislative framework: A review. *Aerosol Sci. Technol.* **2012**, *46*, 719–749. [[CrossRef](#)]

3. Giechaskiel, B.; Lähde, T.; Suarez-Bertoa, R.; Clairotte, M.; Grigoratos, T.; Zardini, A.; Perujo, A.; Martini, G. Particle number measurements in the European legislation and future JRC activities. *Combust. Engines* **2018**, *174*, 3–16. [[CrossRef](#)]
4. Giechaskiel, B.; Joshi, A.; Ntziachristos, L.; Dilara, P. European regulatory framework and particulate matter emissions of gasoline light-duty vehicles: A review. *Catalysts* **2019**, *9*, 586. [[CrossRef](#)]
5. Giechaskiel, B.; Drossinos, Y. Theoretical investigation of volatile removal efficiency of particle number measurement systems. *SAE Int. J. Engines* **2010**, *3*, 1140–1151. [[CrossRef](#)]
6. Burtscher, H. Physical characterization of particulate emissions from diesel engines: A review. *J. Aerosol Sci.* **2005**, *36*, 896–932. [[CrossRef](#)]
7. Giechaskiel, B.; Bonnel, P.; Perujo, A.; Dilara, P. Solid particle number (SPN) portable emissions measurement systems (PEMS) in the European legislation: A review. *IJERPH* **2019**, *16*, 4819. [[CrossRef](#)]
8. Giechaskiel, B.; Vanhanen, J.; Väkevää, M.; Martini, G. Investigation of vehicle exhaust sub-23 nm particle emissions. *Aerosol Sci. Technol.* **2017**, *51*, 626–641. [[CrossRef](#)]
9. Johnson, K.C.; Durbin, T.D.; Jung, H.; Chaudhary, A.; Cocker, D.R.; Herner, J.D.; Robertson, W.H.; Huai, T.; Ayala, A.; Kittelson, D. Evaluation of the European PMP methodologies during on-road and chassis dynamometer testing for dpf equipped heavy-duty diesel vehicles. *Aerosol Sci. Technol.* **2009**, *43*, 962–969. [[CrossRef](#)]
10. Giechaskiel, B.; Manfredi, U.; Martini, G. Engine exhaust solid sub-23 nm particles: I. literature survey. *SAE Int. J. Fuels Lubr.* **2014**, *7*, 950–964. [[CrossRef](#)]
11. Rönkkö, T.; Virtanen, A.; Kannosto, J.; Keskinen, J.; Lappi, M.; Pirjola, L. Nucleation mode particles with a nonvolatile core in the exhaust of a heavy duty diesel vehicle. *Environ. Sci. Technol.* **2007**, *41*, 6384–6389. [[CrossRef](#)]
12. Giechaskiel, B. Solid particle number emission factors of Euro VI heavy-duty vehicles on the road and in the laboratory. *IJERPH* **2018**, *15*, 304. [[CrossRef](#)] [[PubMed](#)]
13. Mayer, A.; Czerwinski, J.; Kasper, M.; Ulrich, A.; Mooney, J.J. *Metal Oxide Particle Emissions from Diesel and Petrol Engines*; SAE: Warrendale, PA, USA, 2012.
14. Giechaskiel, B.; Martini, G. Engine exhaust solid sub-23 nm particles: II feasibility study for particle number measurement systems. *SAE Int. J. Fuels Lubr.* **2014**, *7*, 935–949. [[CrossRef](#)]
15. Giechaskiel, B.; Mamakos, A.; Woodburn, J.; Szczotka, A.; Bielaczyc, P. Evaluation of a 10 nm particle number portable emissions measurement system (PEMS). *Sensors* **2019**, *19*, 5531. [[CrossRef](#)] [[PubMed](#)]
16. Giechaskiel, B.; Lähde, T.; Gandi, S.; Keller, S.; Kreutziger, P.; Mamakos, A. Assessment of 10-nm particle number (PN) portable emissions measurement systems (PEMS) for future regulations. *IJERPH* **2020**, *17*, 3878. [[CrossRef](#)] [[PubMed](#)]
17. Abdul-Khalek, I.S.; Kittelson, D.B. Real time measurement of volatile and solid exhaust particles using a catalytic stripper. *SAE Trans.* **1995**, *104*, 462–478. [[CrossRef](#)]
18. Twigg, M.V. Catalytic control of emissions from cars. *Catal. Today* **2011**, *163*, 33–41. [[CrossRef](#)]
19. Roy, S.; Baiker, A. NO_x storage–reduction catalysis: From mechanism and materials properties to storage–reduction performance. *Chem. Rev.* **2009**, *109*, 4054–4091. [[CrossRef](#)]
20. Liu, G.; Gao, P.-X. A review of NO_x storage/reduction catalysts: Mechanism, materials and degradation studies. *Catal. Sci. Technol.* **2011**, *1*, 552–568. [[CrossRef](#)]
21. Xu, F.; Chen, L.; Stone, R. Effects of a catalytic volatile particle remover (VPR) on the particulate matter emissions from a direct injection spark ignition engine. *Environ. Sci. Technol.* **2011**, *45*, 9036–9043. [[CrossRef](#)]
22. Lobo, P.; Durdina, L.; Brem, B.T.; Crayford, A.P.; Johnson, M.P.; Smallwood, G.J.; Siegerist, F.; Williams, P.I.; Black, E.A.; Llamedo, A.; et al. Comparison of standardized sampling and measurement reference systems for aircraft engine non-volatile particulate matter emissions. *J. Aerosol Sci.* **2020**, *145*, 105557. [[CrossRef](#)]
23. Lin, Y.; Bahreini, R.; Zimmerman, S.; Fofie, E.A.; Asa-Awuku, A.; Park, K.; Lee, S.-B.; Bae, G.-N.; Jung, H.S. Investigation of ambient aerosol effective density with and without using a catalytic stripper. *Atmos. Environ.* **2018**, *187*, 84–92. [[CrossRef](#)]
24. Burtscher, H.; Baltensperger, U.; Bukowiecki, N.; Cohn, P.; Hüglin, C.; Mohr, M.; Matter, U.; Nyeki, S.; Schmatloch, V.; Streit, N.; et al. Separation of volatile and non-volatile aerosol fractions by thermodesorption: Instrumental development and applications. *J. Aerosol Sci.* **2001**, *32*, 427–442. [[CrossRef](#)]

25. Huffman, J.A.; Ziemann, P.J.; Jayne, J.T.; Worsnop, D.R.; Jimenez, J.L. Development and characterization of a fast-stepping/scanning thermodenuder for chemically-resolved aerosol volatility measurements. *Aerosol Sci. Technol.* **2008**, *42*, 395–407. [[CrossRef](#)]
26. Donahue, N.M.; Kroll, J.H.; Pandis, S.N.; Robinson, A.L. A two-dimensional volatility basis set—Part 2: Diagnostics of organic-aerosol evolution. *Atmos. Chem. Phys.* **2012**, *12*, 615–634. [[CrossRef](#)]
27. Maricq, M.M. Chemical characterization of particulate emissions from diesel engines: A review. *J. Aerosol Sci.* **2007**, *38*, 1079–1118. [[CrossRef](#)]
28. Choi, S.; Myung, C.L.; Park, S. Review on characterization of nano-particle emissions and PM morphology from internal combustion engines: Part 2. *Int. J. Autom. Technol.* **2014**, *15*, 219–227. [[CrossRef](#)]
29. Khalek, I.A. Sampling system for solid and volatile exhaust particle size, number, and mass emissions. *SAE Trans.* **2007**, *116*, 122–133. [[CrossRef](#)]
30. Khalek, I.A.; Bougher, T. Development of a solid exhaust particle number measurement system using a catalytic stripper technology. *SAE Int. J. Engines* **2011**, *4*, 610–618. [[CrossRef](#)]
31. Kittelson, D.B.; Stenitzer, M. A new catalytic stripper for removal of volatile particles. In Proceedings of the 7th ETH Conference on Combustion Generated Nanoparticles, Zurich, Switzerland, 18–20 August 2003.
32. Swanson, J.; Kittelson, D. Evaluation of thermal denuder and catalytic stripper methods for solid particle measurements. *J. Aerosol Sci.* **2010**, *41*, 1113–1122. [[CrossRef](#)]
33. Amanatidis, S.; Ntziachristos, L.; Giechaskiel, B.; Katsaounis, D.; Samaras, Z.; Bergmann, A. Evaluation of an oxidation catalyst (“catalytic stripper”) in eliminating volatile material from combustion aerosol. *J. Aerosol Sci.* **2013**, *57*, 144–155. [[CrossRef](#)]
34. Giechaskiel, B.; Zardini, A.; Martini, G. Particle emission measurements from L-category vehicles. *SAE Int. J. Engines* **2015**, *8*, 2322–2337. [[CrossRef](#)]
35. Amanatidis, S.; Ntziachristos, L.; Karjalainen, P.; Saukko, E.; Simonen, P.; Kuittinen, N.; Aakko-Saksa, P.; Timonen, H.; Rönkkö, T.; Keskinen, J. Comparative performance of a thermal denuder and a catalytic stripper in sampling laboratory and marine exhaust aerosols. *Aerosol Sci. Technol.* **2018**, *52*, 420–432. [[CrossRef](#)]
36. Melas, A.D.; Koidi, V.; Deloglou, D.; Daskalos, E.; Zarvalis, D.; Papaioannou, E.; Konstandopoulos, A.G. Development and evaluation of a catalytic stripper for the measurement of solid ultrafine particle emissions from internal combustion engines. *Aerosol Sci. Technol.* **2020**, *54*, 704–714. [[CrossRef](#)]
37. Giechaskiel, B.; Riccobono, F.; Bonnel, P. *Feasibility Study on the Extension of the Real-Driving Emissions (RDE) Procedure to Particle Number (PN): Chassis Dynamometer Evaluation of Portable Emission Measurement Systems (PEMS) to Measure Particle Number (PN) Concentration: Phase II*; Publications Office: Luxembourg, 2015; ISBN 978-92-79-51003-8.
38. Otsuki, Y.; Tochino, S.; Kondo, K.; Haruta, K. *Portable Emissions Measurement System for Solid Particle Number Including Nanoparticles Smaller than 23 nm*; SAE International: Warrendale, PA, USA, 2017.
39. Otsuki, Y.; Takeda, K.; Haruta, K.; Mori, N. *A Solid Particle Number Measurement System Including Nanoparticles Smaller than 23 Nanometers*; SAE International: Warrendale, PA, USA, 2014.
40. Kiwull, B.; Wolf, J.C.; Niessner, R. *Evaluation of Volatile Particle Remover Devices for Exhaust Particle Quantification*; Technische Universität München: Munich, Germany, 2015.
41. Zheng, Z.; Johnson, K.C.; Liu, Z.; Durbin, T.D.; Hu, S.; Huai, T.; Kittelson, D.B.; Jung, H.S. Investigation of Solid Particle Number Measurement: Existence and Nature of Sub-23nm Particles Under PMP Methodology. *J. Aerosol Sci.* **2011**, *42*, 883–897. [[CrossRef](#)]
42. Kasper, M. *Characterisation of the Second Generation PMP “Golden Instrument”*; SAE International: Warrendale, PA, USA, 2008.
43. Giechaskiel, B.; Carriero, M.; Martini, G.; Krasenbrink, A.; Scheder, D. Calibration and validation of various commercial particle number measurement systems. *SAE Int. J. Fuels Lubr.* **2009**, *2*, 512–530. [[CrossRef](#)]
44. Swanson, J.; Kittelson, D.; Giechaskiel, B.; Bergmann, A.; Twigg, M. A miniature catalytic stripper for particles less than 23 nanometers. *SAE Int. J. Fuels Lubr.* **2013**, *6*, 542–551. [[CrossRef](#)]
45. Emery Oil Removal Efficiency. Available online: <http://catalytic-instruments.com/wp-content/uploads/2019/09/Application-note0007.pdf> (accessed on 24 June 2020).
46. Crayford, A.P.; Johnson, M.; Marsh, R.; Sevcenco, Y.; Walters, D.; Williams, P.; Christie, S.; Chung, W.; Petzold, A.; Ibrahim, A.; et al. *SAMPLE III (SC01): Contribution to Aircraft Engine PM Certification Requirement and Standard First Specific Contract—Final Report*; EASA: Cologne, Germany, 2011.

47. Kim, S.; Kondo, K.; Otsuki, Y.; Haruta, K. *A New On-Board PN Analyzer for Monitoring the Real-Driving Condition*; SAE International: Warrendale, PA, USA, 2017.
48. Ho, J.; Kournikakis, B.; Gunning, A.; Fildes, J. Submicron aerosol characterization of water by a differential mobility particle sizer. *J. Aerosol Sci.* **1988**, *19*, 1425–1428. [[CrossRef](#)]
49. Giechaskiel, B.; Chirico, R.; DeCarlo, P.F.; Clairrotte, M.; Adam, T.; Martini, G.; Heringa, M.F.; Richter, R.; Prevot, A.S.H.; Baltensperger, U. Evaluation of the particle measurement programme (PMP) protocol to remove the vehicles' exhaust aerosol volatile phase. *Sci. Total Environ.* **2010**, *408*, 5106–5116. [[CrossRef](#)]
50. Giechaskiel, B. Differences between tailpipe and dilution tunnel sub-23 nm nonvolatile (solid) particle number measurements. *Aerosol Sci. Technol.* **2019**, *53*, 1012–1022. [[CrossRef](#)]
51. Mamakos, A.; Martini, G.; Marotta, A.; Manfredi, U. Assessment of different technical options in reducing particle emissions from gasoline direct injection vehicles. *J. Aerosol Sci.* **2013**, *63*, 115–125. [[CrossRef](#)]
52. Ntziachristos, L.; Amanatidis, S.; Samaras, Z.; Giechaskiel, B.; Bergmann, A. Use of a catalytic stripper as an alternative to the original PMP measurement protocol. *SAE Int. J. Fuels Lubr.* **2013**, *6*, 532–541. [[CrossRef](#)]
53. Mamakos, A.; Martini, G.; Manfredi, U. Assessment of the legislated particle number measurement procedure for a Euro 5 and a Euro 6 compliant diesel passenger cars under regulated and unregulated conditions. *J. Aerosol Sci.* **2013**, *55*, 31–47. [[CrossRef](#)]
54. Giechaskiel, B.; Riccobono, F.; Mendoza-Villafuerte, P.; Grigoratos, T. *Particle Number (PN)—Portable Emissions Measurement Systems (PEMS) Heavy Duty Vehicles Evaluation Phase at the Joint Research Centre (JRC)*; Publications Office: Luxembourg, 2016.
55. Zheng, Z.; Durbin, T.D.; Karavalakis, G.; Johnson, K.C.; Chaudhary, A.; Cocker, D.R.; Herner, J.D.; Robertson, W.H.; Huai, T.; Ayala, A.; et al. Nature of sub-23-nm particles downstream of the European particle measurement programme (PMP)-compliant system: A real-time data perspective. *Aerosol Sci. Technol.* **2012**, *46*, 886–896. [[CrossRef](#)]
56. Ntziachristos, L.; Giechaskiel, B.; Pistikopoulos, P.; Samaras, Z. *Comparative Assessment of Two Different Sampling Systems for Particle Emission Type-Approval Measurements*; SAE International: Warrendale, PA, USA, 2005.
57. Giechaskiel, B. Particle number emissions of a diesel vehicle during and between regeneration events. *Catalysts* **2020**. [[CrossRef](#)]
58. Yu, F. Effect of ammonia on new particle formation: A kinetic H₂SO₄-H₂O-NH₃ nucleation model constrained by laboratory measurements. *J. Geophys. Res.* **2006**, *111*. [[CrossRef](#)]
59. Lemmetty, M.; Vehkamäki, H.; Virtanen, A.; Kulmala, M.; Keskinen, J. Homogeneous ternary H₂SO₄-NH₃-H₂O nucleation and diesel exhaust: A classical approach. *Aerosol Air Qual. Res.* **2007**, *7*, 489–499. [[CrossRef](#)]
60. Benson, D.R.; Yu, J.H.; Markovich, A.; Lee, S.-H. Ternary homogeneous nucleation of H₂SO₄, NH₃, and H₂O under conditions relevant to the lower troposphere. *Atmos. Chem. Phys.* **2011**, *11*, 4755–4766. [[CrossRef](#)]
61. Suarez-Bertoa, R.; Pechout, M.; Vojtišek, M.; Astorga, C. Regulated and non-regulated emissions from Euro 6 diesel, gasoline and CNG vehicles under real-world driving conditions. *Atmosphere* **2020**, *11*, 204. [[CrossRef](#)]
62. Czerwinski, J.; Zimmerli, Y.; Mayer, A.; Heeb, N.; Lemaire, J.; D'Urbano, G.; Bunge, R. *Testing of Combined DPF+SCR Systems for HD-Retrofitting—VERTdePN*; SAE International: Warrendale, PA, USA, 2009.
63. Sipilä, M.; Berndt, T.; Petaja, T.; Brus, D.; Vanhanen, J.; Stratmann, F.; Patokoski, J.; Mauldin, R.L.; Hyvarinen, A.-P.; Lihavainen, H.; et al. The role of sulfuric acid in atmospheric nucleation. *Science* **2010**, *327*, 1243–1246. [[CrossRef](#)]
64. Uhrner, U.; von Löwis, S.; Vehkamäki, H.; Wehner, B.; Bräsel, S.; Hermann, M.; Stratmann, F.; Kulmala, M.; Wiedensohler, A. Dilution and aerosol dynamics within a diesel car exhaust plume—CFD simulations of on-road measurement conditions. *Atmos. Environ.* **2007**, *41*, 7440–7461. [[CrossRef](#)]
65. Olin, M.; Alanen, J.; Palmroth, M.R.T.; Rönkkö, T.; Dal Maso, M. Inversely modeling homogeneous H₂SO₄—H₂O nucleation rate in exhaust-related conditions. *Atmos. Chem. Phys.* **2019**, *19*, 6367–6388. [[CrossRef](#)]
66. Karjalainen, P.; Rönkkö, T.; Pirjola, L.; Heikkilä, J.; Happonen, M.; Arnold, F.; Rothe, D.; Bielaczyc, P.; Keskinen, J. Sulfur driven nucleation mode formation in diesel exhaust under transient driving conditions. *Environ. Sci. Technol.* **2014**, *2336*–2343. [[CrossRef](#)] [[PubMed](#)]
67. Du, H.; Yu, F. Nanoparticle formation in the exhaust of vehicles running on ultra-low sulfur fuel. *Atmos. Chem. Phys.* **2008**, *8*, 4729–4739. [[CrossRef](#)]

68. Vaaraslahti, K.; Keskinen, J.; Giechaskiel, B.; Solla, A.; Murtonen, T.; Vesala, H. Effect of lubricant on the formation of heavy-duty diesel exhaust nanoparticles. *Environ. Sci. Technol.* **2005**, *39*, 8497–8504. [[CrossRef](#)]
69. Lemmetty, M.; Rönkkö, T.; Virtanen, A.; Keskinen, J.; Pirjola, L. The effect of sulphur in diesel exhaust aerosol: Models compared with measurements. *Aerosol Sci. Technol.* **2008**, *42*, 916–929. [[CrossRef](#)]
70. Khalek, I.A.; Kittelson, D.B.; Brear, F. *Nanoparticle Growth During Dilution and Cooling of Diesel Exhaust: Experimental Investigation and Theoretical Assessment*; SAE International: Warrendale, PA, USA, 2000.
71. Arnold, F.; Pirjola, L.; Rönkkö, T.; Reichl, U.; Schlager, H.; Lähde, T.; Heikkilä, J.; Keskinen, J. First online measurements of sulfuric acid gas in modern heavy-duty diesel engine exhaust: Implications for nanoparticle formation. *Environ. Sci. Technol.* **2012**, *46*, 11227–11234. [[CrossRef](#)]
72. Vouitsis, E.; Ntziachristos, L.; Samaras, Z. Modelling of diesel exhaust aerosol during laboratory sampling. *Atmos. Environ.* **2005**, *39*, 1335–1345. [[CrossRef](#)]
73. Vouitsis, E.; Ntziachristos, L.; Samaras, Z. Theoretical investigation of the nucleation mode formation downstream of diesel after-treatment devices. *Aerosol Air Qual. Res.* **2008**, *8*, 37–53. [[CrossRef](#)]
74. Yamada, H.; Funato, K.; Sakurai, H. Application of the PMP methodology to the measurement of sub-23 nm solid particles: Calibration procedures, experimental uncertainties, and data correction methods. *J. Aerosol Sci.* **2015**, *88*, 58–71. [[CrossRef](#)]
75. Giechaskiel, B.; Martini, G. JRC sub-23 nm update. In Proceedings of the 37th PMP meeting, Brussels, Belgium, 7 October 2015.
76. AVL Comments on GTR15 Amendment. Available online: <https://wiki.unece.org/display/trans/PMP+Web+Conference+02+April> (accessed on 24 June 2020).
77. Neyestanaki, A.K.; Klingstedt, F.; Salmi, T.; Murzin, D.Y. Deactivation of postcombustion catalysts, a review. *Fuel* **2004**, *83*, 395–408. [[CrossRef](#)]
78. Giechaskiel, B.; Ntziachristos, L.; Samaras, Z.; Casati, R.; Scheer, V.; Vogt, R. *Effect of Speed and Speed-Transition on the Formation of Nucleation Mode Particles from a Light Duty Diesel Vehicle*; SAE International: Warrendale, PA, USA, 2007.
79. Cooper, B.J.; Thoss, J.E. Role of NO in diesel particulate emission control. *SAE Trans.* **1989**, *98*, 612–624. [[CrossRef](#)]
80. Kröcher, O.; Widmer, M.; Elsener, M.; Rothe, D. Adsorption and desorption of SO_x on diesel oxidation catalysts. *Ind. Eng. Chem. Res.* **2009**, *48*, 9847–9857. [[CrossRef](#)]
81. Li, L.; King, D.L. Method for determining performance of sulfur oxide adsorbents for diesel emission control using online measurements of SO₂ and SO₃ in the effluent. *Ind. Eng. Chem. Res.* **2004**, *43*, 4452–4456. [[CrossRef](#)]
82. Koutsopoulos, S.; Rasmussen, S.B.; Eriksen, K.M.; Fehrmann, R. The role of support and promoter on the oxidation of sulfur dioxide using platinum based catalysts. *Appl. Catal. A Gen.* **2006**, *306*, 142–148. [[CrossRef](#)]
83. Xue, E.; Seshan, K.; van Ommen, J.G.; Ross, J.R.H. Catalytic control of diesel engine particulate emission: Studies on model reactions over a EuroPt-1 (Pt/SiO₂) catalyst. *Appl. Catal. B Environ.* **1993**, *2*, 183–197. [[CrossRef](#)]
84. Wyatt, M.; Manning, W.A.; Roth, S.A.; D’Aniello, M.J.; Andersson, E.S.; Fredholm, S.C.G. The design of flow-through diesel oxidation catalysts. *SAE Trans.* **1993**, *102*, 211–223. [[CrossRef](#)]
85. Horiuchi, M.; Saito, K.; Ichihara, S. The effects of flow-through type oxidation catalysts on the particulate reduction of 1990’s diesel engines. *SAE Trans.* **1990**, *99*, 1268–1278. [[CrossRef](#)]
86. Hamzehlouyan, T.; Sampara, C.; Li, J.; Kumar, A.; Epling, W. Experimental and kinetic study of SO₂ oxidation on a Pt/γ-Al₂O₃ catalyst. *Appl. Catal. B Environ.* **2014**, *152*, 108–116. [[CrossRef](#)]
87. Koltsakis, G. Catalytic automotive exhaust aftertreatment. *Prog. Energy Combust. Sci.* **1997**, *23*, 1–39. [[CrossRef](#)]
88. Mathieu, Y.; Tzanis, L.; Soulard, M.; Patarin, J.; Vierling, M.; Molière, M. Adsorption of SO_x by oxide materials: A review. *Fuel Process. Technol.* **2013**, *114*, 81–100. [[CrossRef](#)]
89. Smedler, G.; Ahlström, G.; Fredholm, S.; Frost, J.; Löf, P.; Marsh, P.; Walker, A.; Winterborn, D. *High Performance Diesel Catalysts for Europe Beyond 1996*; SAE International: Warrendale, PA, USA, 1995.
90. Henk, M.G.; Williamson, W.B.; Silver, R.G. *Diesel Catalysts for Low Particulate and Low Sulfate Emissions*; SAE International: Warrendale, PA, USA, 1992.
91. Lampert, J.; Kazi, M.; Farrauto, R. Palladium catalyst performance for methane emissions abatement from lean burn natural gas vehicles. *Appl. Catal. B Environ.* **1997**, *14*, 211–223. [[CrossRef](#)]

92. Kärkkäinen, M.; Honkanen, M.; Viitanen, V.; Kolli, T.; Valtanen, A.; Huuhtanen, M.; Kallinen, K.; Vippola, M.; Lepistö, T.; Lahtinen, J.; et al. Deactivation of diesel oxidation catalysts by sulphur in laboratory and engine-bench scale aging. *Top Catal.* **2013**, *56*, 672–678. [[CrossRef](#)]
93. Taylor, K.C. Sulfur storage on automotive catalysts. *Ind. Eng. Chem. Prod. Res. Dev.* **1976**, *15*, 264–268. [[CrossRef](#)]
94. Wang, Q.; Zhu, J.; Wei, S.; Chung, J.S.; Guo, Z. Sulfur poisoning and regeneration of NO_x storage–reduction Cu/K₂Ti₂O₅ catalyst. *Ind. Eng. Chem. Res.* **2010**, *49*, 7330–7335. [[CrossRef](#)]
95. Liu, X.; Chen, L.; Qi, G. Enhanced SO₂ capture performance of MnO₂ by doping with alkali metal ions for diesel emission control. *Chem. Eng. Technol.* **2018**, *41*, 1675–1681. [[CrossRef](#)]
96. Li, L.; King, D.L. High-capacity sulfur dioxide absorbents for diesel emissions control. *Ind. Eng. Chem. Res.* **2005**, *44*, 168–177. [[CrossRef](#)]
97. Horiuchi, M.; Saito, K.; Ichihara, S. *Sulfur Storage and Discharge Behavior on Flow-Through Type Oxidation Catalysts*; SAE International: Warrendale, PA, USA, 1991.
98. Centi, G.; Passarini, N.; Perathoner, S.; Riva, A. Combined DeSO_x/DeNO_x reactions on a copper on alumina sorbent-catalyst. 1. Mechanism of sulfur dioxide oxidation-adsorption. *Ind. Eng. Chem. Res.* **1992**, *31*, 1947–1955. [[CrossRef](#)]
99. Limousy, L.; Mahzoul, H.; Brillhac, J.F.; Gilot, P.; Garin, F.; Maire, G. SO₂ sorption on fresh and aged SO_x traps. *Appl. Catal. B Environ.* **2003**, *42*, 237–249. [[CrossRef](#)]
100. Dawody, J.; Skoglundh, M.; Olsson, L.; Fridell, E. Sulfur deactivation of Pt/SiO₂, Pt/BaO/Al₂O₃, and BaO/Al₂O₃ NO_x storage catalysts: Influence of SO₂ exposure conditions. *J. Catal.* **2005**, *234*, 206–218. [[CrossRef](#)]
101. Dawody, J.; Skoglundh, M.; Olsson, L.; Fridell, E. Kinetic modelling of sulfur deactivation of Pt/BaO/Al₂O₃ and BaO/Al₂O₃ NO_x storage catalysts. *Appl. Catal. B Environ.* **2007**, *70*, 179–188. [[CrossRef](#)]
102. Kylhammar, L.; Carlsson, P.-A.; Ingelsten, H.H.; Grönbeck, H.; Skoglundh, M. Regenerable ceria-based SO_x traps for sulfur removal in lean exhausts. *Appl. Catal. B Environ.* **2008**, *84*, 268–276. [[CrossRef](#)]
103. Hamzehlouyan, T.; Sampara, C.S.; Li, J.; Kumar, A.; Epling, W.S. Kinetic study of adsorption and desorption of SO₂ over γ -Al₂O₃ and Pt/ γ -Al₂O₃. *Appl. Catal. B Environ.* **2016**, *181*, 587–598. [[CrossRef](#)]
104. Yoshida, K.; Asanuma, T.; Nishioka, H.; Hayashi, K.; Hirota, S. *Development of NO_x Reduction System for Diesel Aftertreatment with Sulfur Trap Catalyst*; SAE International: Warrendale, PA, USA, 2007.
105. Englund, J.; Xie, K.; Dahlin, S.; Schaefer, A.; Jing, D.; Shwan, S.; Andersson, L.; Carlsson, P.-A.; Pettersson, L.J.; Skoglundh, M. Deactivation of a Pd/Pt bimetallic oxidation catalyst used in a biogas-powered Euro VI heavy-duty engine installation. *Catalysts* **2019**, *9*, 1014. [[CrossRef](#)]
106. Argyle, M.; Bartholomew, C. Heterogeneous catalyst deactivation and regeneration: A review. *Catalysts* **2015**, *5*, 145–269. [[CrossRef](#)]
107. Chasapidis, L.; Melas, A.D.; Tsakis, A.; Zarvalis, D.; Konstandopoulos, A. *A Sampling and Conditioning Particle System for Solid Particle Measurements Down to 10 nm*; SAE International: Warrendale, PA, USA, 2019.
108. Miller, J.; Jin, L. *Global Progress toward Soot-Free Diesel Vehicles*; International Council Clean Transportation (ICCT) Report; ICCT: Washington, DC, USA, 2019.
109. Yamada, H.; Inomata, S.; Tanimoto, H. Mechanisms of increased particle and VOC emissions during DPF active regeneration and practical emissions considering regeneration. *Environ. Sci. Technol.* **2017**, *51*, 2914–2923. [[CrossRef](#)] [[PubMed](#)]
110. Yasar, A.; Haider, R.; Tabinda, A.B.; Kausar, F.; Khan, M. A comparison of engine emissions from heavy, medium, and light vehicles for CNG, diesel, and gasoline fuels. *Pol. J. Environ. Stud.* **2013**, *22*, 1277–1281.
111. Tavares, J.R.; Sthel, M.S.; Campos, L.S.; Rocha, M.V.; Lima, G.R.; da Silva, M.G.; Vargas, H. Evaluation of pollutant gases emitted by ethanol and gasoline powered vehicles. *Proc. Environ. Sci.* **2011**, *4*, 51–60. [[CrossRef](#)]
112. Gentner, D.R.; Worton, D.R.; Isaacman, G.; Davis, L.C.; Dallmann, T.R.; Wood, E.C.; Herndon, S.C.; Goldstein, A.H.; Harley, R.A. Chemical composition of gas-phase organic carbon emissions from motor vehicles and implications for ozone production. *Environ. Sci. Technol.* **2013**, *47*, 11837–11848. [[CrossRef](#)]
113. Tobias, H.J.; Beving, D.E.; Ziemann, P.J.; Sakurai, H.; Zuk, M.; McMurry, P.H.; Zarling, D.; Waytulonis, R.; Kittelson, D.B. Chemical analysis of diesel engine nanoparticles using a nano-DMA/thermal desorption particle beam mass spectrometer. *Environ. Sci. Technol.* **2001**, *35*, 2233–2243. [[CrossRef](#)]

114. Sakurai, H.; Tobias, H.J.; Park, K.; Zarling, D.; Docherty, K.S.; Kittelson, D.B.; McMurry, P.H.; Ziemann, P.J. On-line measurements of diesel nanoparticle composition and volatility. *Atmos. Environ.* **2003**, *37*, 1199–1210. [[CrossRef](#)]
115. Swanson, J.J.; Kittelson, D.B.; Watts, W.F.; Gladis, D.D.; Twigg, M.V. Influence of storage and release on particle emissions from new and used CRTs. *Atmos. Environ.* **2009**, *43*, 3998–4004. [[CrossRef](#)]
116. Schneider, J.; Hock, N.; Weimer, S.; Borrmann, S.; Kirchner, U.; Vogt, R.; Scheer, V. Nucleation particles in diesel exhaust: Composition inferred from in situ mass spectrometric analysis. *Environ. Sci. Technol.* **2005**, *39*, 6153–6161. [[CrossRef](#)]
117. Karavalakis, G.; Gysel, N.; Schmitz, D.A.; Cho, A.K.; Sioutas, C.; Schauer, J.J.; Cocker, D.R.; Durbin, T.D. Impact of biodiesel on regulated and unregulated emissions, and redox and proinflammatory properties of PM emitted from heavy-duty vehicles. *Sci. Total Environ.* **2017**, *584*, 1230–1238. [[CrossRef](#)]
118. Alves, C.A.; Lopes, D.J.; Calvo, A.I.; Evtugina, M.; Rocha, S.; Nunes, T. Emissions from light-duty diesel and gasoline in-use vehicles measured on chassis dynamometer test cycles. *Aerosol Air Qual. Res.* **2015**, *15*, 99–116. [[CrossRef](#)]
119. Tsai, J.-H.; Huang, P.-H.; Chiang, H.-L. Air pollutants and toxic emissions of various mileage motorcycles for ECE driving cycles. *Atmos. Environ.* **2017**, *153*, 126–134. [[CrossRef](#)]
120. Ntziachristos, L.; Vonk, W.A.; Papadopoulos, G.; van Mensch, P.; Geivanidis, S.; Mellios, G.; Papadimitriou, G.; Steven, H.; Elstgeest, M.; Ligterink, N.E.; et al. *Effect Study of the Environmental Step Euro 5 for L-Category Vehicles*; European Commission: Brussels, Belgium, 2017; ISBN 978-92-79-70203-7.
121. Kontses, A.; Ntziachristos, L.; Zardini, A.A.; Papadopoulos, G.; Giechaskiel, B. Particulate emissions from L-Category vehicles towards Euro 5. *Environ. Res.* **2020**, *182*, 109071. [[CrossRef](#)]
122. Costagliola, M.A.; Murena, F.; Prati, M.V. Exhaust emissions of volatile organic compounds of powered two-wheelers: Effect of cold start and vehicle speed. Contribution to greenhouse effect and tropospheric ozone formation. *Sci. Total Environ.* **2014**, *468*, 1043–1049. [[CrossRef](#)]
123. Liu, X.; Deng, B.; Fu, J.; Xu, Z.; Liu, J.; Li, M.; Li, Q.; Ma, Z.; Feng, R. The effect of air/fuel composition on the HC emissions for a twin-spark motorcycle gasoline engine: A wide condition range study. *Chem. Eng. J.* **2019**, *355*, 170–180. [[CrossRef](#)]
124. Szymlet, N.; Lijewski, P.; Sokolnicka, B.; Siedlecki, M.; Domowicz, A. Analysis of research method, results and regulations regarding the exhaust emissions from two-wheeled vehicles under actual operating conditions. *J. Ecol. Eng.* **2020**, *21*, 128–139. [[CrossRef](#)]
125. Kašpar, J.; Fornasiero, P.; Hickey, N. Automotive catalytic converters: Current status and some perspectives. *Catal. Today* **2003**, *77*, 419–449. [[CrossRef](#)]
126. Jaworski, A.; Maździel, M.; Lejda, K. Creating an emission model based on portable emission measurement system for the purpose of a roundabout. *Environ. Sci. Pollut. Res.* **2019**, *26*, 21641–21654. [[CrossRef](#)]
127. Zhu, G.; Liu, J.; Fu, J.; Xu, Z.; Guo, Q.; Zhao, H. Experimental study on combustion and emission characteristics of turbocharged gasoline direct injection (GDI) engine under cold start new European driving cycle (NEDC). *Fuel* **2018**, *215*, 272–284. [[CrossRef](#)]
128. Yang, Z.; Liu, Y.; Wu, L.; Martinet, S.; Zhang, Y.; Andre, M.; Mao, H. Real-world gaseous emission characteristics of Euro 6b light-duty gasoline- and diesel-fueled vehicles. *Transp. Res. Part D Transp. Environ.* **2020**, *78*, 102215. [[CrossRef](#)]
129. Ma, C.; Wu, L.; Mao, H.; Fang, X.; Wei, N.; Zhang, J.; Yang, Z.; Zhang, Y.; Lv, Z.; Yang, L. Transient characterization of automotive exhaust emission from different vehicle types based on on-road measurements. *Atmosphere* **2020**, *11*, 64. [[CrossRef](#)]
130. Simonen, P.; Kalliokoski, J.; Karjalainen, P.; Rönkkö, T.; Timonen, H.; Saarikoski, S.; Aurela, M.; Bloss, M.; Triantafyllopoulos, G.; Kontses, A.; et al. Characterization of laboratory and real driving emissions of individual Euro 6 light-duty vehicles—Fresh particles and secondary aerosol formation. *Environ. Pollut.* **2019**, *255*, 113175. [[CrossRef](#)]
131. Ko, J.; Son, J.; Myung, C.-L.; Park, S. Comparative study on low ambient temperature regulated/unregulated emissions characteristics of idling light-duty diesel vehicles at cold start and hot restart. *Fuel* **2018**, *233*, 620–631. [[CrossRef](#)]
132. Bikas, G.; Zervas, E. Regulated and non-regulated pollutants emitted during the regeneration of a diesel particulate filter. *Energy Fuels* **2007**, *21*, 1543–1547. [[CrossRef](#)]

133. Jung, S.; Lim, J.; Kwon, S.; Jeon, S.; Kim, J.; Lee, J.; Kim, S. Characterization of particulate matter from diesel passenger cars tested on chassis dynamometers. *J. Environ. Sci.* **2017**, *54*, 21–32. [[CrossRef](#)]
134. R'Mili, B.; Boréave, A.; Meme, A.; Vernoux, P.; Leblanc, M.; Noël, L.; Raux, S.; D'Anna, B. Physico-chemical characterization of fine and ultrafine particles emitted during diesel particulate filter active regeneration of Euro 5 diesel vehicles. *Environ. Sci. Technol.* **2018**, *52*, 3312–3319. [[CrossRef](#)]
135. Ruehl, C.; Smith, J.D.; Ma, Y.; Shields, J.E.; Burnitzki, M.; Sobieralski, W.; Ianni, R.; Chernich, D.J.; Chang, M.-C.O.; Collins, J.F.; et al. Emissions during and real-world frequency of heavy-duty diesel particulate filter regeneration. *Environ. Sci. Technol.* **2018**, *52*, 5868–5874. [[CrossRef](#)] [[PubMed](#)]
136. Giechaskiel, B.; Gioria, R.; Carriero, M.; Lähde, T.; Forloni, F.; Perujo, A.; Martini, G.; Bissi, L.M.; Terenghi, R. Emission factors of a Euro VI heavy-duty diesel refuse collection vehicle. *Sustainability* **2019**, *11*, 1067. [[CrossRef](#)]
137. Doozandegan, M.; Hosseini, V.; Ehteram, M.A. Solid nanoparticle and gaseous emissions of a diesel engine with a diesel particulate filter and use of a high-sulphur diesel fuel and a medium-sulphur diesel fuel. *Proc. Inst. Mech. Eng. Part. D J. Automob. Eng.* **2017**, *231*, 941–951. [[CrossRef](#)]
138. Rothe, D.; Knauer, M.; Emmerling, G.; Deyerling, D.; Niessner, R. Emissions during active regeneration of a diesel particulate filter on a heavy duty diesel engine: Stationary tests. *J. Aerosol Sci.* **2015**, *90*, 14–25. [[CrossRef](#)]
139. Smith, J.D.; Ruehl, C.; Burnitzki, M.; Sobieralski, W.; Ianni, R.; Quiros, D.; Hu, S.; Chernich, D.; Collins, J.; Huai, T.; et al. Real-time particulate emissions rates from active and passive heavy-duty diesel particulate filter regeneration. *Sci. Total Environ.* **2019**, *680*, 132–139. [[CrossRef](#)] [[PubMed](#)]



© 2020 by the authors. Licensee MDPI, Basel, Switzerland. This article is an open access article distributed under the terms and conditions of the Creative Commons Attribution (CC BY) license (<http://creativecommons.org/licenses/by/4.0/>).